

LAF3, a Novel Factor Required for Normal Phytochrome A Signaling^{1[w]}

Peter D. Hare, Simon G. Møller, Li-Fang Huang, and Nam-Hai Chua*

Laboratory of Plant Molecular Biology, The Rockefeller University, 1230 York Avenue, New York 10021 (P.D.H., S.G.M., L.-F.H., N.-H.C.); and Department of Biology, University of Leicester, University Road, Leicester LE1 7RH, United Kingdom (S.G.M.)

Phytochrome A (phyA) is the photolabile plant light receptor that mediates broad spectrum very low-fluence responses and high irradiance responses to continuous far-red light (FR_c). An Arabidopsis mutant *laf3-1* (long after far-red 3) was recovered from a screen for transposon-tagged mutants that exhibit reduced inhibition of hypocotyl elongation in FR_c. The *laf* phenotype correlated well with a strongly attenuated disappearance of *XTR7* transcript in FR_c. The effects of *laf3-1* on phyA-controlled *CAB*, *CHS*, and *PET H* expression were more subtle, and the mutation had no clear effects on *PET E* and *ASN1* transcript levels in FR_c. The use of two alternative transcription initiation sites in the *LAF3* gene generates two isoforms that differ only at their N termini. Transcripts encoding both isoforms were induced during germination and were present at slightly higher levels in de-etiolated seedlings than in those grown in darkness. No significant differential regulation of the two isoforms was observed upon exposure to either FR_c or continuous red light. Transcripts encoding the shorter isoform (LAF3_{ISF2}) always appear to be more abundant than those encoding the longer isoform (LAF3_{ISF1}). However, both isoforms were capable of full complementation of the *laf3-1* hypocotyl phenotype in FR_c. When fused to a yellow fluorescent protein, both isoforms localize to the perinuclear region, suggesting that *LAF3* encodes a product that might regulate nucleo-cytoplasmic trafficking of an intermediate(s) involved in phyA signal transduction.

Phytochromes are soluble chromoproteins that regulate plant growth and development by their ability to interconvert between two stable spectral forms. Red light (R) converts the R-absorbing Pr form (the form synthesized in darkness) to the Pfr (far-red absorbing form) and far-red light (FR) reconverts Pfr to Pr. Two important features distinguish phytochrome A (phyA) from the other four phytochromes in Arabidopsis. First, although the Arabidopsis phytochromes phyB to phyE are activated exclusively by R and inactivated by irradiation with FR, phyA can be activated by FR and low fluences of R and blue light (B). Secondly, although phyA levels decrease rapidly after exposure to light as a result of both down-regulation of *PHYA* gene transcription (Cantón and Quail, 1999) and far greater photolability of phyA than other phytochromes (Sharrock and Clack, 2002), phyA is by far the most abundant phytochrome in etiolated seedlings. These features enable phyA to perform a seminal role in triggering the shift between skotomorphogenesis and photomorphogenesis. Together, they ensure that the inhibition of hypocotyl elongation, and the activation of physio-

logical changes needed to ensure photosynthetic competence are already underway when seedlings emerge from the soil surface. Despite its lability in light-grown plants, the influence of phyA throughout the life cycle is evidenced by its involvement in sensing photoperiod to ensure that flowering is initiated at the proper time (Johnson et al., 1994; Yanovsky and Kay, 2002) and its requirement in mature plants for activation of the *psbD* promoter by B (Thum et al., 2001).

Extensive changes in gene expression underlie the dramatic shift between etiolated seedling growth and photomorphogenesis (Ma et al., 2001). Expression profiling also suggests that phyA initiates photomorphogenesis primarily by rapidly targeting the promoters of a set of transcription factors, which are in turn responsible for initiating a cascade of transcriptional induction or repression events (Tepperman et al., 2001). This conceivably enables orchestration of the expression of multiple downstream target genes in a highly branched signal transduction network that permits integration of phyA inputs with other environmental cues and endogenous developmental signals (Møller et al., 2002; Wang et al., 2002). Our current insight into the cell biology of phytochrome signaling (Møller et al., 2002) further validates the importance of regulated gene expression in phyA action. Although phyA appears to reside exclusively in the cytoplasm of seedlings grown in darkness, conditions known to activate phyA responses trigger a rapid translocation of some, but not all, phyA into the nucleus (Nagy and Schäfer, 2002). Considerable

¹ This work was supported by NIH grant GM 44640, a JST (CREST) grant, a grant from the Biotechnology and Biological Science Research Council (S.G.M.), and by the South African National Research Foundation (postdoctoral fellowship to P.D.H.).

[w] The online version of this article contains Web-only data.

* Corresponding author; e-mail chua@rockefeller.edu; fax 212-327-8327.

Article, publication date, and citation information can be found at <http://www.plantphysiol.org/cgi/doi/10.1104/pp.103.028480>.

interest centers around the likely importance of the association of nuclear phyA with light-dependent transcriptional complexes (Fairchild et al., 2000), and it seems likely that the regulation of phyA localization may be critical to many aspects of phyA activity. The nuclear localization of COP1, a repressor of photomorphogenesis, also appears to be important for its role in targeting photomorphogenesis-promoting factors such as HY5 and LAF1 for degradation (von Arnim et al., 1997; Osterlund et al., 2000; Seo et al., 2003).

Although the majority of intermediates currently known to be essential for normal seedling responsiveness to activated phyA are predicted to localize to the nucleus (Hoecker et al., 1999; Hudson et al., 1999; Fairchild et al., 2000; Soh et al., 2000; Ballesteros et al., 2001; Dieterle et al., 2001; Wang and Deng, 2002), others are found exclusively in the cytoplasm (Bolle et al., 2000; Hsieh et al., 2000; Guo et al., 2001) or in both compartments (Choi et al., 1999; Desnos et al., 2001; Zeidler et al., 2001). Plastidic events (Møller et al., 2001) and peroxisomal processes (Hu et al., 2002) also contribute to an intact phyA signaling network. Most of the factors known to be essential for phyA signaling appear to be soluble proteins. There is presently little insight into the functional relationships between these signaling intermediates or the role of the majority of activated phyA that remains in the cytoplasm, even under conditions that are optimal for nuclear translocation (Nagy and Schäfer, 2002). Our insight into how these intermediates might relate to the apparent importance of phyA's protein kinase activity (Yeh and Lagarias, 1998; Fankhauser et al., 1999; C6lon-Carmona et al., 2000; Kim et al., 2002), the involvement of G proteins and fairly ubiquitous secondary messengers (Bowler et al., 1994; Guo et al., 2001; Kang et al., 2001), and the likely importance of protein degradation in regulating phyA-triggered photomorphogenesis (Dieterle et al., 2001) is also extremely limited. A more global view of the hierarchical arrangement of the intermediates and how closely they act within the phyA signaling network is likely to remain refractory until additional players in the phyA signaling pathway are identified.

Against this background, we have continued to search for mutants specifically compromised in the inhibition of hypocotyl elongation in continuous far-red light (FR_c), but which are unaffected in the phyA-mediated block of greening in white (W) light after pre-irradiation with FR_c (Barnes et al., 1996a). Here, we report characterization of a *laf* (long after far-red) mutant defective in a protein (LAF3) that is located in the nuclear periphery. LAF3 encodes two isoforms with homology to a conserved family of bacterial proteins. The subcellular localization of LAF3 and fairly selective misregulation of phyA-controlled genes associated with its loss suggests that LAF3 participates in transmission of certain aspects of the phyA signal from the site of phyA activation in the cytoplasm of etiolated seedlings to the promoters of

the genes that define certain downstream targets of activated phyA.

RESULTS

laf3-1 Is Impaired in phyA Signaling

A collection of Arabidopsis Ds-tagged lines (Sundaresan et al., 1995) was screened for reduced inhibition of hypocotyl elongation in FR_c and one mutant, *laf3-1* (long after far red 3), possessed longer hypocotyls under both low and high fluences of FR_c, but no significant hypocotyl elongation phenotype in darkness or continuous red light (R_c), B, or W light (Fig. 1A). This indicates that the role of the LAF3 locus in inhibiting hypocotyl elongation is specific to the phyA photoreceptor (Fig. 1A). Under both fluences of FR_c tested, *laf3-1* hypocotyl lengths were always intermediate between those observed in WT and *phyA* null mutant seedlings, indicating a partial loss of responsiveness to FR_c and no significant fluence dependence.

PCR analysis of a backcross-derived F₂ population of 120 plants indicated that the *laf3-1* hypocotyl phenotype cosegregated with kanamycin resistance conferred by a single Ds element and was inherited in a Mendelian fashion consistent with the presence of a single recessive mutation. The abundance of phyA is an important determinant of the sensitivity of seedling photomorphogenesis in FR_c. Immunoblot analysis of WT and *laf3-1* seedlings grown in darkness indicated that levels of phyA are not compromised in etiolated *laf3-1* seedlings (Fig. 1C). Furthermore, the relatively slow disappearance of phyA in FR_c to a steady-state level is comparable between *laf3-1* and *Ler* (Fig. 1C). Therefore, the reduced responsiveness of *laf3-1* to FR_c does not result from a lower level of phyA in etiolated *laf3-1* seedlings or from reduced rates of phyA degradation in FR_c.

Arabidopsis seedlings with an intact phyA signaling pathway initiate chloroplast development in FR_c but chloroplasts undergo photobleaching after subsequent W light treatment. In contrast, the *phyA*, *fhy1/pat3*, *fhy3*, and *pat1* mutants are insensitive to this block of greening (Barnes et al., 1996a; Bolle et al., 2000). Germination and growth of *laf3-1* and WT seedlings at very low fluences of FR_c (0.4 μmol m⁻² s⁻¹) indicated that *laf3-1* seedlings showed similar FR-induced photobleaching characteristics as WT seedlings (data not shown). Moreover, defects in apical hook opening, cotyledon expansion, and loss of negative gravitropism are not apparent in *laf3-1*, even at low fluences of FR_c (data not shown).

Gene expression analysis indicated that of six phyA-regulated transcripts tested, *laf3-1* was most strongly affected in FR_c-mediated disappearance of a transcript encoding a xyloglucan endotransglycosylase-related protein (*XTR7*). However, *XTR7* levels in FR_c-irradiated *laf3-1* seedlings were intermediate between those found in WT and *phyA* back-

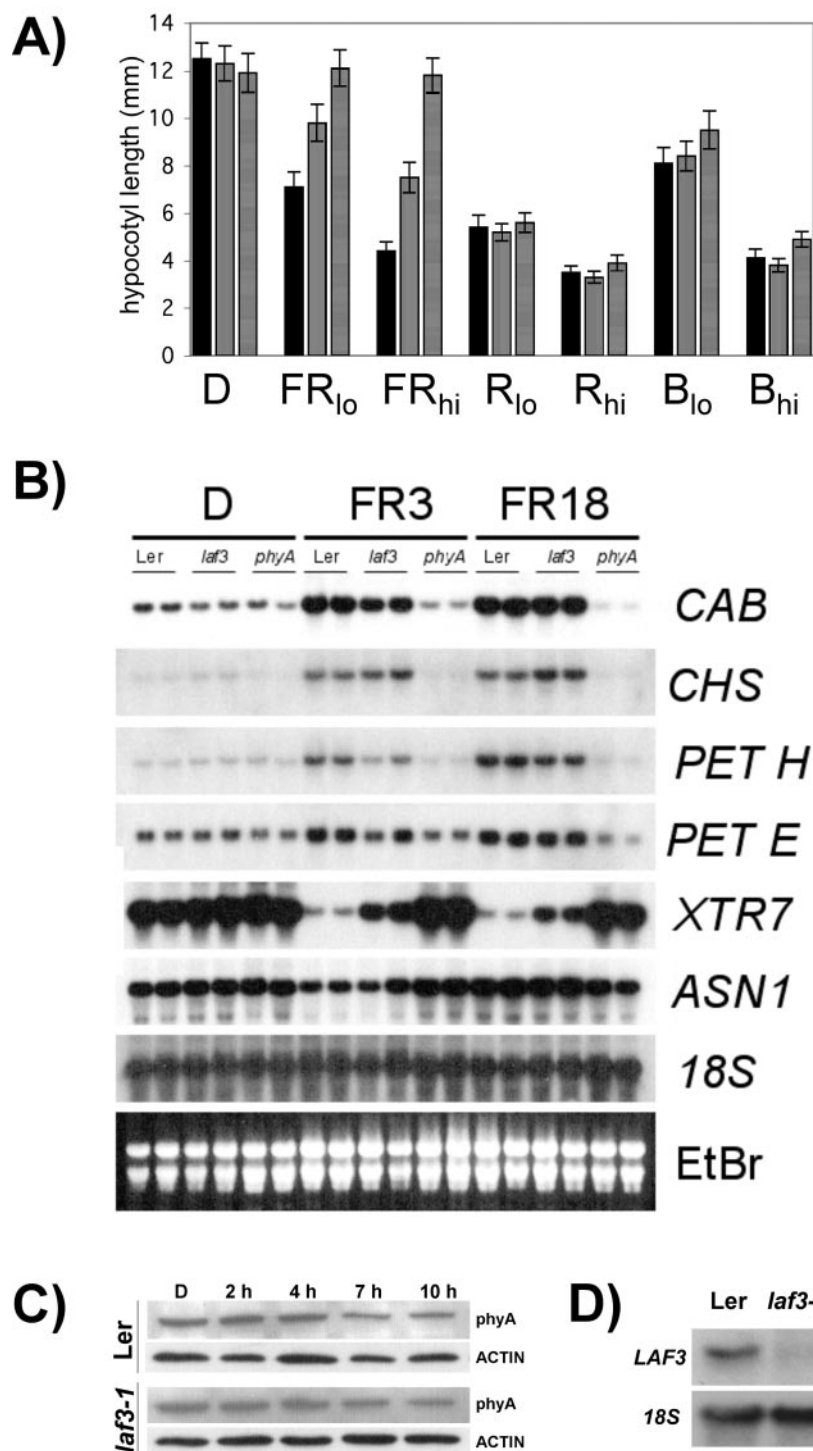


Figure 1. Seedling phenotypes of *laf3-1*. A, Hypocotyl lengths of wild-type (WT; Landsberg *erecta* [*Ler*], solid bars), *laf3-1* (vertical stripes), and *phyA-201* (horizontal stripes) seedlings in darkness (D) and after irradiation with FR_c (FR₁₀, 2.1 $\mu\text{mol m}^{-2} \text{s}^{-1}$; FR₁₈, 6.3 $\mu\text{mol m}^{-2} \text{s}^{-1}$), R (R₁₀, 10.1 $\mu\text{mol m}^{-2} \text{s}^{-1}$; R₁₈, 27.4 $\mu\text{mol m}^{-2} \text{s}^{-1}$), and B (B₁₀, 2.3 $\mu\text{mol m}^{-2} \text{s}^{-1}$; B₁₈, 9.4 $\mu\text{mol m}^{-2} \text{s}^{-1}$) light. Hypocotyl lengths were measured after 4 d of growth under the indicated light condition. Values are means \pm SD ($n \geq 80$). All measurements were repeated at least three times with comparable results. B, Northern-blot analysis of phyA-regulated genes in WT (*Ler*), *laf3-1*, and *phyA*. Total RNA was harvested from 4-d-old seedlings grown in darkness, without exposure to FR (D) or after 3 h (FR3) or 18 h (FR18) irradiation with FR_c (3.9 $\mu\text{mol m}^{-2} \text{s}^{-1}$). Each lane contained 15 μg of total RNA. Duplicate samples for each treatment were from seedlings grown independently under identical conditions. The same blot was probed for transcripts encoding *CAB*, *CHS*, *PET H*, *PET E*, *XTR7*, and *ASN1*. Ethidium bromide staining and hybridization with an 18S rRNA probe are shown as loading controls. C, Western analysis of phyA abundance in 4-d-old etiolated *laf3-1* and *Ler* seedlings without prior exposure to light (D) or after 2, 4, 7, or 10 h of exposure to FR_c (5.3 $\mu\text{mol m}^{-2} \text{s}^{-1}$). The mAA1 antibody did not detect any phyA protein (approximately 120 kD) in the *phyA-201* null mutant (data not shown; Shinomura et al., 1996). A single band recognized by an actin antibody (approximately 45 kD) indicates comparable total protein levels. D, *laf3-1* possesses severely reduced levels of *LAF3* transcript. A 1.3-kb cDNA probe corresponding to the 3' ends of both *LAF3* isoforms was used to detect the combined levels of both transcripts in 10-d-old light-grown seedlings.

grounds (Fig. 1B). The effects of *laf3-1* on FR_c-stimulated increases in transcripts encoding *CAB* (chlorophyll *a/b*-binding) protein and ferredoxin: NADP(H) oxidoreductase (*PET H*) abundance were more subtle. Surprisingly, *CHS* (chalcone synthase) transcript levels in *laf3-1* were slightly more elevated than in WT seedlings after both 3 and 18 h of exposure to FR_c (Fig. 1B). The *laf3-1* mutation had no clear

effects on either plastocyanin (*PET E*) or Asn synthetase (*ASN1*) transcript levels in FR_c.

The *laf3-1* mutation does not appear to have any obvious developmental or morphological manifestations in mature plants. Under extended short-day conditions (8 h of high-intensity fluorescent light, 8 h of low-intensity incandescent light, and 8 h of darkness), the flowering time of *laf3-1* plants and the

number of leaves at the time of bolting were not significantly different from WT (data not shown). This was in sharp contrast to *phyA* mutants that showed delayed flowering under the same conditions (Johnson et al., 1994; Yanovsky and Kay, 2002).

LAF3 Encodes Two Isoforms with Homology to a Conserved Family of Bacterial Proteins

The flanking region of the gene disrupted by the *Ds* insertion in *laf3-1* was cloned using inverse PCR. A database search using the TBLAST algorithm, and the tagged sequence as the query input indicated that the *Ds* element was inserted within an intron of a predicted open reading frame (ORF) near the bottom of Arabidopsis chromosome 3 (At3g55850 on bacterial artificial chromosome F27K19 in the vicinity of the marker SGCSNP86). Northern-blot analysis of *laf3-1* and WT seedlings demonstrated substantially reduced levels of total LAF3 transcript (Fig. 1D). Thus far, no other mutations causing an FR-specific long-hypocotyl phenotype are found in the vicinity of the LAF3 locus. The only other locus on chromosome 3 implicated specifically in *phyA* signaling is *FHY3* (Wang and Deng, 2002), found more than 12.9 Mb from LAF3. Screening of a flower cDNA library (Weigel et al., 1992) using this flanking region as a probe enabled isolation of a 1.3-kb cDNA that was complete at the 3' end.

Interestingly, 5'-RACE analysis revealed that two isoforms of the LAF3 gene product are expressed in Arabidopsis seedlings. Neither isoform is identical to the gene product predicted by annotation of the Arabidopsis genome. Although the start codon of the first isoform (LAF3_{ISF1}; 583 amino acids; accession no. AY295343) has been predicted correctly, the acceptor site of the second intron was predicted incorrectly, and the transcript encoding LAF3_{ISF1} contains 15 introns (Fig. 2A) instead of 14 introns. The transcription start site and start codon of the second isoform (LAF3_{ISF2}; 576 amino acids; accession no. AY295344) both occur within the first intron of the ORF encoding LAF3_{ISF1} (Fig. 2A). Because there is an in-frame fusion of the first eight amino acids of LAF3_{ISF2} to the codon for Ala-16 of LAF3_{ISF1} and all other introns are identically spliced, the two isoforms differ only in the first few N-terminal amino acids. Transcription start sites for both isoforms are preceded by putative TATA boxes TATAAAT and TTATTT, which are found 43 and 101 bp upstream of the transcription start sites of LAF3_{ISF1} and LAF3_{ISF2}, respectively. Database searches also indicated a single LAF3 cDNA in Arabidopsis (accession no. AY057597) that encodes LAF3_{ISF2}. No coding regions are predicted to lie within the 3-kb upstream region of LAF3_{ISF1} or within the 3-kb downstream region of either isoform; moreover, no expressed sequence tags have been identified in these regions.

Sequence analysis did not reveal any extensive regions of similarity within either isoform with known

protein domains, although several bacterial and archaeal hydrolases bear strong similarity only to an amino-terminal region of LAF3 indicated in Figure 2C. Both isoforms are predicted to contain a membrane-spanning region at their N termini (Fig. 2B). Interestingly, this is predicted to occur in the region where both proteins differ partly in their amino acid sequence. The LAF3 isoforms show closest similarity to a predicted rice gene product (554 amino acids; accession no. BAB64699) that is approximately 59% identical to the Arabidopsis LAF3_{ISF1} protein and, moreover, is predicted to contain a transmembrane helical region between Phe-7 and Leu-21. Curiously, the only other homologs in the database are from 45 different bacteria and the lower eukaryotes *Neurospora crassa* and *Leishmania major*. The only homolog for which any function is known is that from *Pectobacterium carotovora*, for which the LAF3 homolog is encoded by the *aepA* (activator of extracellular protein production A) locus. An *aepA*⁻ knockout in this soft rot bacterium (previously in the genus *Erwinia*) was associated with reduced phytopathogenicity associated with coordinated down-regulation of genes encoding cell wall-degrading enzymes such as pectate lyase, polygalacturonase, cellulose, and protease (Liu et al., 1993). The molecular masses of these proteins range from 42 to 76 kD (both Arabidopsis LAF3 isoforms are around 63 kD) with an average of 59 kD. The estimated pI values of the 48 proteins range from 4.4 to 8.7 with an average pI of 5.9. The pIs of the Arabidopsis LAF3 isoforms are approximately 5.3. When compared with the LAF3_{ISF1} isoform, amino acid identities range between approximately 30% for the *Deinococcus radiodurans*, *Novosphingobium aromaticivorans*, *Ralstonia metallidurans*, *Halobacterium* sp. NRC-1, *Thermoanaerobacter tengcongensis*, *Chloroflexus aurantiacus*, and *Bacillus halodurans* homologs to around 17% for *Aquifex aeolicus*. There appear to be no homologs in animals. The homology between these proteins is likely to be significant because after alignment of all 48 homologs with LAF3_{ISF1}, the LAF3_{ISF1} residues His-389, His-421, and Asp-485 displayed complete conservation; residues His-113, His-115, Gly-264, Gly-342, and Gly-542 were conserved in all but one of the homologs; and Pro-107, Pro-182, and Ala-550 were conserved in all but two homologs (all numbers pertain to LAF3_{ISF1}; a complete alignment is provided as Supplemental Data available in the online version of this article at <http://www.plantphysiol.org>). An additional 11 residues of both Arabidopsis LAF3 isoforms were conserved in more than 85% of the 48 homologs, and another 20 residues displayed conservation in more than 70% of the proteins.

Genetic Complementation of *laf3-1*

To confirm that the *laf3-1* phenotype resulted from a single transposon insertion and to test whether only

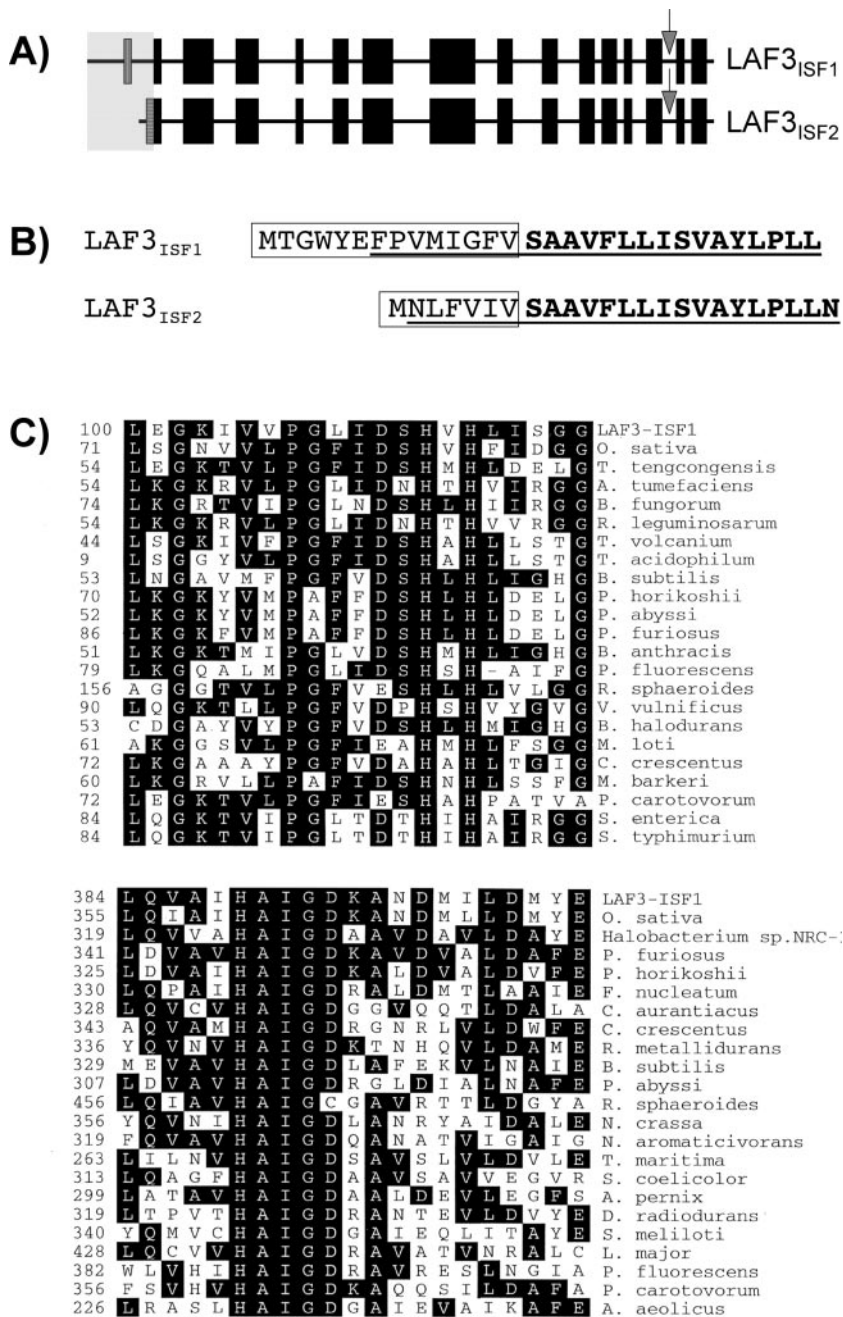


Figure 2. A, Schematic representation of both coding regions of the *LAF3* gene deduced from the comparison between the genomic sequence (accession no. AL163832) and cDNA sequences determined by RACE and reverse transcriptase (RT)-PCR. Black boxes, Exons encoding identical regions in isoforms. The transcription start site and start codon of *LAF3*_{ISF2} occur within the first intron of the primary *LAF3*_{ISF1} transcript, giving rise to isoforms differing in their N termini. The unique N termini of *LAF3*_{ISF1} and *LAF3*_{ISF2} are indicated by vertical and horizontal shading, respectively. The site of the transposon insertion in *laf3-1* in the 14th intron of the *LAF3*_{ISF1} ORF and 13th intron of the *LAF3*_{ISF2} ORF is indicated by an arrow. B, Divergent N-terminal stretches of both *LAF3* isoforms are boxed. Regions which are predicted to be transmembrane domains using five independent algorithms are underlined. Remarkably, the first portions of these regions span N-terminal stretches where the two isoforms are encoded by different DNA templates. Amino acids encoded by the same exon are in bold. Default parameters were used for the TMHMM (<http://www.cbs.dtu.dk/services/TMHMM>), PHDhtm (<http://www.embl-heidelberg.de/predictprotein>), HMMtop (<http://www.enzim.hu/hmmtop>), TM-Pred (<http://www.ch.embnet.org>), and PSORT (<http://psort.nibb.ac.jp>) algorithms to predict transmembrane helices in the N termini of both *LAF3* isoforms. Transmembrane segments predicted by the individual programs were considered overlapping if 12 or more amino acids were shared by all predicted segments. C, Alignment of two highly conserved regions in both *LAF3* isoforms with homologous regions of putative proteins from rice (*Oryza sativa*), bacteria, and lower eukaryotes. Accession numbers of sequences and a complete alignment of *LAF3*_{ISF1} with 48 homologs are provided in Supplemental Data.

one or both of the *LAF3* isoforms are required for an intact phyA signal transduction pathway, we tested the ability of three constructs to complement the *laf3-1* hypocotyl phenotype in FR_c. First, *laf3-1* mutants were transformed with an 8,067-bp genomic fragment extending from 3,050 bp upstream of the start codon of *LAF3*_{ISF1} to 1,293 bp downstream of the stop codon of both isoforms. Of 23 T₁ transformants, four transgenic lines displayed partial complementation (Fig. 3). The frequency of complementation was greater in *laf3-1* mutants transformed with the 35S::*LAF3*_{ISF1} and 35S::*LAF3*_{ISF2} constructs, in which expression of both isoforms was under con-

trol of the CaMV 35S promoter. Of 65 35S::*LAF3*_{ISF1} transformants tested, 42 were indistinguishable from WT plants after 4 d of FR_c light treatment, and of 63 35S::*LAF3*_{ISF2} transformants tested, 33 displayed clear complementation (Fig. 3). The greater efficacy of CaMV 35S-regulated transcription in complementing the mutant in comparison with the endogenous promoter suggests that possibly additional regulatory regions outside of the 3 kb upstream of the start codon or an additional factor(s), e.g. chromosomal modification of the *LAF3* promoter, might normally regulate *LAF3* expression.

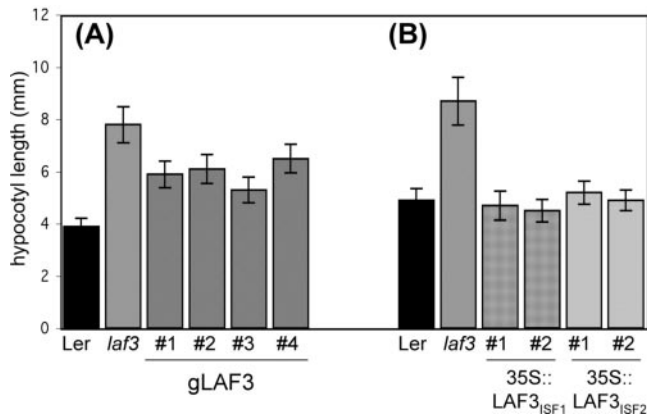


Figure 3. Expression of *LAF3* restores the WT hypocotyl phenotype to *laf3-1* mutant seedlings. A, Hypocotyl lengths of WT (*Ler* -0), *laf3-1*, and four independent transgenic *laf3-1* lines (T_3 generation) expressing the gLAF3 construct. The fluence of FR_c was $5.7 \mu\text{mol m}^{-2} \text{s}^{-1}$. B, Hypocotyl lengths of WT (*Ler* -0), *laf3-1*, and transgenic *laf3-1* lines (T_2 generation) expressing either the *LAF3*_{ISF1} or *LAF3*_{ISF2} cDNA under the control of the cauliflower mosaic virus (CaMV) 35S promoter. The fluence of FR_c was $4.3 \mu\text{mol m}^{-2} \text{s}^{-1}$. For all experiments, values are means \pm SD ($n \geq 80$). Hypocotyl lengths were measured after 4 d of growth in darkness or FR_c .

Both Isoforms of LAF3 Localize in the Perinuclear Region

Preliminary studies involving transient expression of *LAF3*_{ISF1}-yellow fluorescent protein (YFP) and *LAF3*_{ISF2}-YFP fusions in onion (*Allium cepa*) epidermal cells indicated that both isoforms were targeted to the nuclear periphery with no significant fluorescence within the cytoplasm, nucleus, or cell periphery (data not shown). The same preferential perinuclear distribution was observed when *LAF3*_{ISF1}-YFP and *LAF3*_{ISF2}-YFP were constitutively expressed under the control of CaMV 35S in *laf3-1* seedlings (Fig. 4). There was no evidence of fluorescence in the cortical endoplasmic reticulum, and visualization

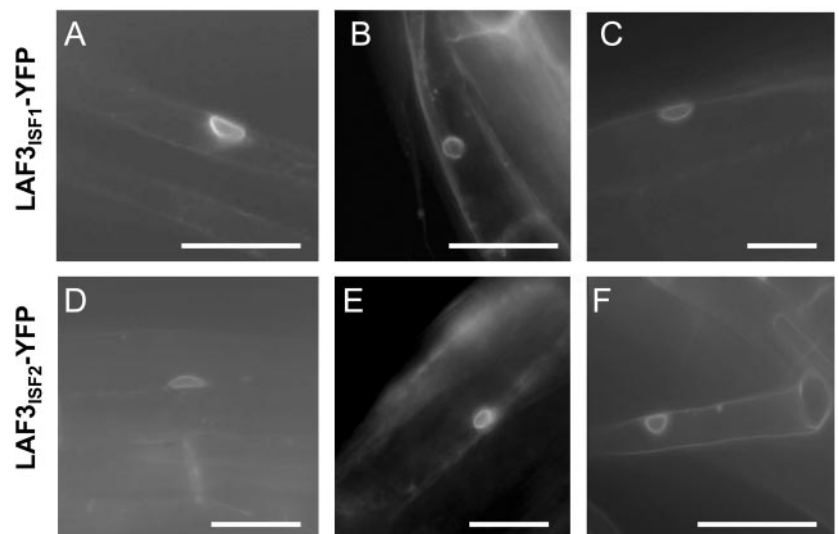
with both cyan fluorescent protein and YFP filters suggested that any signal associated with the plasma membrane was artifactual. Irradiation with light did not affect the subcellular distribution of either *LAF3* fusion in etiolated seedlings. Fusion of either isoform to the N terminus of YFP did not significantly affect the ability of both isoforms to complement the *laf3-1* phenotype (data not shown).

Expression of *LAF3* Transcripts

Preliminary northern-blot analysis using a probe incapable of distinguishing between both isoforms suggested that an approximately 2-kb *LAF3* transcript was detected at highly reduced levels in *laf3-1* compared with WT seedlings (Fig. 1D). Examination of the tissue-specific regulation of *LAF3* transcripts using the same probe indicated a comparable low level of expression in seedlings grown in W light, rosette leaves, stems, flowers, and siliques, with an approximately 2- to 3-fold higher abundance in roots (data not shown). Examination of the light regulation of *LAF3* expression in WT plants using this probe suggested a slight and relatively slow increase in *LAF3* transcript abundance after irradiation of etiolated seedlings with FR_c (data not shown).

The demonstration that *LAF3* encodes two protein isoforms with distinct N termini introduces the interesting question of whether the choice of *LAF3* transcript initiation site has important regulatory implications for *LAF3* function. To validate the northern-blot analyses and reveal any differential regulation of both isoforms, we employed mimic-controlled RT-PCR analysis. Oligonucleotides were designed to amplify regions encoding the divergent N termini of both isoforms and the first 73 amino acids common to both *LAF3*_{ISF1} and *LAF3*_{ISF2}. The two exogenous standards used in competitive PCR had the same oligonucleotide templates as the target

Figure 4. *LAF3*-YFP localizes to the nuclear periphery in stably transformed *laf3-1* seedlings. A signal with significant enrichment in the nuclear periphery was observed in several independent lines expressing 35S::*LAF3*_{ISF1}-YFP in hypocotyl (A and B) or root (C) cells. The same distribution of signal was observed in lines expressing 35S::*LAF3*_{ISF2}-YFP in hypocotyl (D and E) or root (F) cells. Scale bars = 20 μm .



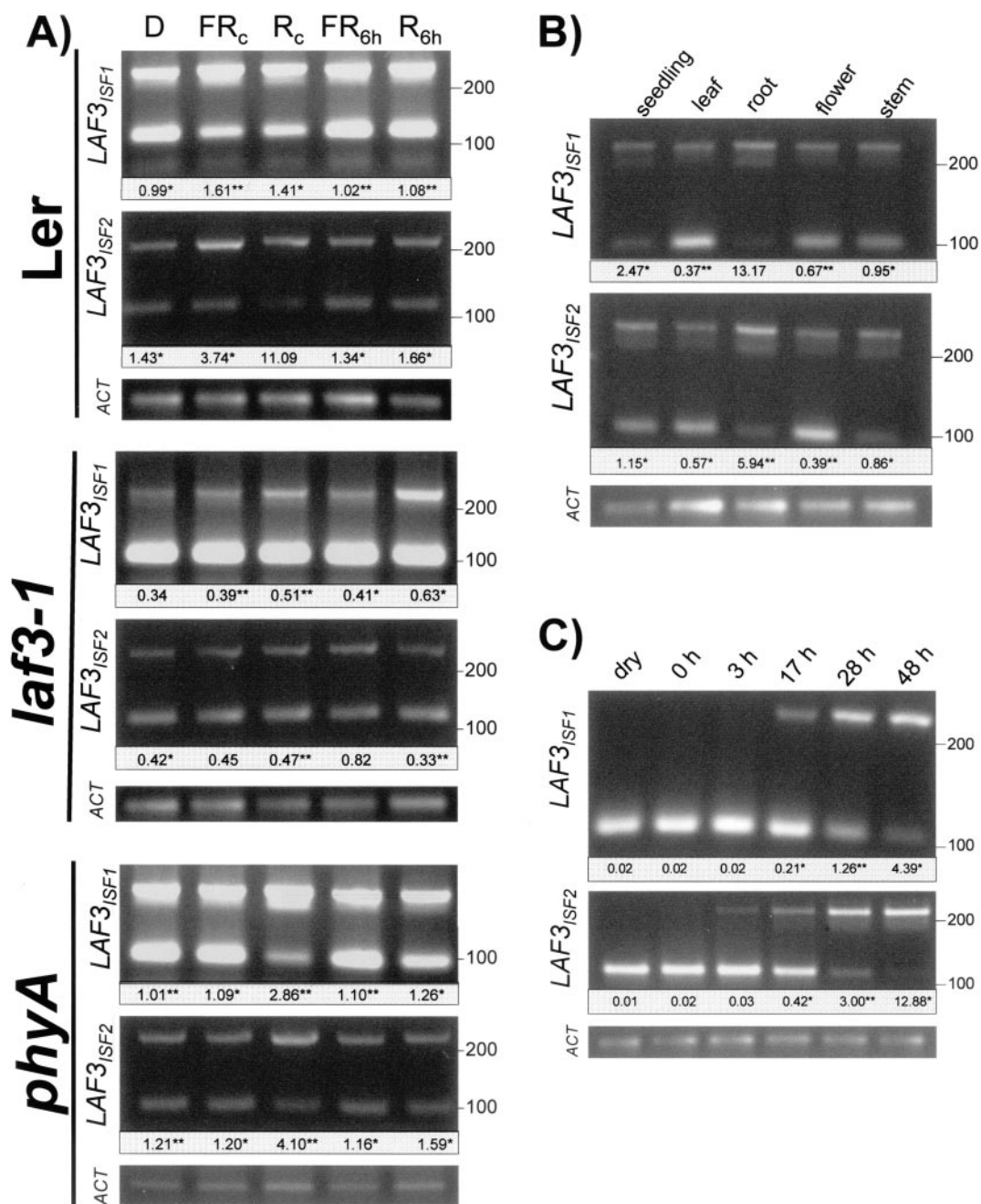


Figure 5. Transcriptional regulation of the *LAF3* gene. Fragments specific to *LAF3* isoforms are both approximately 250 bp, whereas fragments arising from amplification of mimics are 110 bp. Values below each lane indicate the mean ratio (determined from three independent PCRs) of signal arising from amplification of *LAF3* transcript to that arising from amplification of the mimic target. **, SD < 5% of mean ratio; *, SD < 10% of mean ratio. For each RT product, amplification of a fragment specific to *ACTIN2* transcript (*ACT*) confirmed comparable amounts of starting RNA and comparable RT efficiency within all comparisons. A, Relative levels of the *LAF3*_{ISF1} and *LAF3*_{ISF2} transcripts in 4-d-old *Ler*, *laf3-1*, and *phyA* seedlings after continuous growth in darkness (D), FR_c of intensity 4.7 $\mu\text{mol m}^{-1} \text{s}^{-1}$, R_c of intensity 5.1 $\mu\text{mol m}^{-1} \text{s}^{-1}$, growth for 4 d in darkness before a 6-h pulse with 4.7 $\mu\text{mol m}^{-1} \text{s}^{-1}$ FR_c (FR_{6h}), or growth for 4 d in darkness before a 6 h pulse with 5.1 $\mu\text{mol m}^{-1} \text{s}^{-1}$ R_c (R_{6h}). The results indicated were obtained after 22 cycles of PCR containing 10^{-7} pmol *LAF3*_{ISF1} mimic or 10^{-6} pmol *LAF3*_{ISF2} mimic. B, Both *LAF3* transcripts are present at higher levels in roots of mature plants than in 4-d-old seedlings germinated and grown in W light or leaves, flowers, and stems of adult plants. The results indicated (Legend continues on facing page.)

cDNA but generated smaller PCR products than the target DNA. Depending on the relative ratio of mimic to target, one or the other will be amplified preferentially.

Comparison of $LAF3_{ISF1}$ and $LAF3_{ISF2}$ transcript levels in 4-d-old seedlings indicated that transcripts encoding both isoforms were at least 2- to 3-fold higher in seedlings grown in R_c and FR_c than in etiolated seedlings but that 6 h of irradiation with light of either wavelength was inadequate to induce accumulation of either transcript to the level observed in seedlings germinated and grown for 4 d under either monochromatic wavelengths (Fig. 5A). Not surprisingly, induction of accumulation of both transcripts by FR_c displayed an absolute dependence on *phyA*, although a detectable increase in both $LAF3_{ISF1}$ and $LAF3_{ISF2}$ transcripts by R_c treatments indicates that activation of other phytochromes is also adequate to induce accumulation of *LAF3* transcripts (Fig. 5A). Nonetheless, *phyA* does play a significant role in the early phases of induction of *LAF3* transcript accumulation by R_c . Inclusion of *laf3-1* seedlings in this experiment enabled confirmation by RT-PCR that both $LAF3_{ISF1}$ and $LAF3_{ISF2}$ transcript levels are significantly lower in *laf3-1* than in WT seedlings (Fig. 5A). RT-PCR analysis of $LAF3_{ISF1}$ and $LAF3_{ISF2}$ transcript levels in 4-d-old seedlings germinated in W light and roots, rosette leaves, stems, and flowers of mature plants indicated that both transcripts were expressed at the highest levels in roots, with comparable levels in leaves, flowers, and stems and slightly higher levels in seedlings (Fig. 5B). Based on the different concentrations of mimics used for the amplification reactions for each isoform, it appears that $LAF3_{ISF1}$ transcript levels are at least an order of magnitude lower than those of $LAF3_{ISF2}$ in all of the tissue types examined (Fig. 5B).

Given the central role played by *phyA* in regulating germination and early seedling development, we investigated *LAF3* transcript levels in dry seeds, seeds that had been imbibed in darkness at 4°C for 4 d (0-h time point denotes extracts prepared immediately after the end of stratification), and then at four time points after exposure of stratified seeds to continuous W light at 22°C. These spanned the time of radicle emergence (around 24 h) and cotyledon expansion and greening (complete within 48 h of growth in continuous W light at 22°C). In the absence of mimic fragments, neither transcript was detectable in dry seeds or seeds imbibed in darkness, although

both transcripts were present within 3 h after transfer of stratified seeds to germination-promoting conditions (data not shown). As indicated in Figure 5C, levels of both transcripts increased progressively throughout the first 2 d after transfer to continuous W light at 22°C with lower levels of $LAF3_{ISF1}$ than $LAF3_{ISF2}$.

DISCUSSION

Molecular events that signal the availability of light play a central role during plant growth and development. As one of the most critical developmental transitions in the life cycle of flowering plants, seedling photomorphogenesis provides an excellent experimental system to elucidate the components required for light signal transduction. Activation of *phyA* in etiolated seedlings causes cotyledon expansion and greening and inhibition of hypocotyl cell elongation. Despite much recent progress, the molecular basis of these morphological manifestations is still largely unknown. This arises primarily from the difficulty in establishing how known intermediates in *phyA* signaling interact with one another in the context of a transduction network.

The Contribution of *LAF3* to the *phyA* Signaling Network

The specific hyposensitivity of *laf3-1* hypocotyl elongation to FR in comparison with R and B implicates the requirement of *LAF3* for complete responsiveness to activated *phyA*. Defective *LAF3* expression does not affect the inhibition of hypocotyl elongation triggered by activation of any of the other known photoreceptors in Arabidopsis. Clearly, *LAF3* is essential for full response capacity to activated *phyA*, although the map position of *LAF3* excludes the possibility of allelism with any other FR-specific long hypocotyl mutants. Like all known mutants defective in *phyA* signaling intermediates, significantly reduced levels of *LAF3* transcripts do not completely eliminate any of the FR_c -induced seedling responses tested in this study. Furthermore, the absence of any effects of the *laf3-1* mutation on FR_c -regulated hook opening and cotyledon expansion, hypocotyl gravitropism, greening in W light after a prolonged FR_c treatment, *PET E* and *ASN1* regulation, or *phyA*-mediated photoperiod sensing in mature plants indicates that the *LAF3* locus may normally modulate a

Figure 5. (Legend continued from facing page.)

were obtained after 20 cycles of PCR containing either 5×10^{-8} pmol $LAF3_{ISF1}$ mimic or 10^{-7} pmol $LAF3_{ISF2}$ mimic. C, Relative levels of the $LAF3_{ISF1}$ and $LAF3_{ISF2}$ transcripts in dry *Ler* seeds (dry), seeds imbibed at 4°C for 4 d (0 h), and throughout the process of germination (times indicate hours after transfer of imbibed seeds imbibed to continuous W light at 22°C). The intensity of W light was $16 \mu\text{mol m}^{-2} \text{s}^{-1}$. For most seeds, radicle emergence was evident by 24 h and seedling cotyledon opening, and greening was evident by 48 h. The results indicated were obtained after 20 cycles of PCR containing 5×10^{-8} pmol $LAF3_{ISF1}$ mimic or 10^{-7} pmol $LAF3_{ISF2}$ mimic. No amplification was obtained for either of the $LAF3_{ISF1}$ and $LAF3_{ISF2}$ -specific fragments even after 35 cycles of PCR in the absence of a mimic fragment.

more discrete subset of *phyA*-regulated responses than are affected in most mutants deficient in positively acting intermediates in *phyA* signaling (Hudson et al., 1999; Bolle et al., 2000; Fairchild et al., 2000; Fankhauser and Chory, 2000; Hsieh et al., 2000; Soh et al., 2000; Ballesteros et al., 2001; Møller et al., 2001; Wang and Deng, 2002; Wang et al., 2002).

Analysis of *LAF3* transcript levels (Fig. 5) and failure to discern any *LAF3* overexpression phenotype strongly suggest that *LAF3* action is unlikely to be significantly regulated at the transcriptional level. However, we cannot eliminate the possibility that both *LAF3* isoforms may be differentially regulated by light posttranscriptionally. The ubiquitous expression of *LAF3* and the lack of specificity for FR wavelengths to modulate *LAF3* levels might be interpreted as indicating that *LAF3* normally plays a permissive role in *phyA* signaling, although the apparent developmental specificity of the *laf3-1* mutant phenotype argues against a role for *LAF3* in regulating basic housekeeping functions. Although *LAF3* transcripts are higher in roots than in other tissues, and root elongation in FR is inhibited in *phyA* seedlings (Büchle et al., 2000), we failed to observe significant effects of the *laf3* mutation on root elongation in 4-d-old seedlings irradiated with FR_c or on the frequency of lateral root initiation in 14-d-old seedlings grown in continuous W light (data not shown). The use of the CaMV 35S promoter in complementation studies may have obscured a role for one of the two *LAF3* isoforms in mediating *phyA* responses. We cannot eliminate the possibility that when levels of an isoform normally not involved in *phyA* signaling are considerably elevated, it might be capable of fulfilling a role normally attributable to the other isoform. Further investigation of whether such genetic redundancy might occur would require knowledge of the endogenous levels of both isoforms in seedlings. Therefore, the biological significance of the use of alternative transcription initiation sites to generate two isoforms that differ only in their N termini remains enigmatic.

LAF3 Displays a Perinuclear Distribution

Insight into the relationship between *LAF3* and known intermediates in *phyA* signaling might benefit from knowledge of its subcellular localization. It is accepted that *phyA* responses are regulated primarily at the level of altered gene expression. In accordance, two key events involving the movement of signaling components across the nuclear envelope appear to be essential for complete responsiveness to activated *phyA*. The first is the relatively rapid translocation of *phyA* from the cytoplasm to the nucleus triggered by the same light conditions required for *phyA* activation (Nagy and Schäfer, 2002). Here, *phyA* activates waves of transcriptional activation or repression to control the downstream target genes that define discrete branches of the *phyA*-regulated

transcriptional network (Tepperman et al., 2001). The second event is the simultaneous derepression of gene expression that appears to be mediated at least in part by the relatively slow movement of COP1 out of the nucleus (von Arnim et al., 1997). The FR-induced nuclear depletion of COP1 is dependent on *phyA* (Osterlund and Deng, 1998). In addition to these two processes, *phyA* signaling in *Arabidopsis* is also likely to mediate the light-dependent nuclear translocation of transcription factors that are cytoplasmic in darkness (Kircher et al., 1999).

Although we cannot formally exclude the possibility that expression of *LAF3* proteins under the control of the CaMV 35S promoter might cause them to be targeted to a subcellular site different from that of the naturally expressed proteins, our characterization of *LAF3* reiterates the apparent importance of physical separation of cellular processes as a control point in *phyA* signaling (Møller et al., 2002; Nagy and Schäfer, 2002). Intriguingly, the significant enrichment in the abundance of *LAF3* at the nuclear rim closely resembles that reported for SUB1, a cytoplasmic calcium-binding protein that negatively regulates both cryptochrome and *phyA* responses (Guo et al., 2001), although unlike *sub1*, *laf3* does not display a dramatic hypocotyl elongation phenotype in B (Fig. 1A). The *laf3-1* hypocotyl phenotype also appears to display far less fluence dependence than that of *sub1* (Guo et al., 2001). Neither of the *LAF3* isoforms nor SUB1 possess the recently identified WPP domain that appears to be a novel plant motif necessary and sufficient for targeting plant RanGAPs and the plant-specific nuclear envelope-associated MAF1 protein to the nuclear rim (Rose and Meier, 2001). The role of the putative transmembrane domains of both *LAF3* isoforms remains unclear.

It is tempting to speculate that *LAF3* may participate in the *phyA*-dependent translocation of a latent factor(s) across the nuclear envelope from its subcellular location in darkness to a site where it triggers *phyA* responses in the light. Spatial confinement is an excellent mechanism to regulate gene expression by controlled movement of signaling intermediates across the nuclear envelope (Amador et al., 2001; Heerklotz et al., 2001; Igarashi et al., 2001; Carmo-Fonseca, 2002; Stone et al., 2003). Regulated subcellular compartmentation may also be essential for the regulation of posttranslational modifications such as the addition or removal of ligands [e.g. (de)phosphorylation, (de)acetylation, and (de)conjugation with ubiquitin or ubiquitin-like tags] and/or regulation of the stability of gene products. The combined regulation of ligand modification and subcellular localization potentially confers considerable complexity on the regulation of a signaling intermediate. For instance, four different species, each with a distinct function, might be envisaged for a protein that displays nucleocytoplasmic shuttling and can be reversibly conjugated to a regulatory ligand.

Given the comparatively weak phenotype of *laf3-1*, we do not suspect that LAF3 normally acts at the level of the phyA photoreceptor itself. The phyA-specific signaling intermediate FHY1/PAT3 also occurs in both nuclear and cytoplasmic compartments (Desnos et al., 2001; Zeidler et al., 2001), although a significant role for FHY1 in regulating *CHS* and plastocyanin (*PET E*) but not *CAB* transcript abundance in FR_c (Barnes et al., 1996b) contrasts with the role of LAF3 in the regulation of these genes (Fig. 1B). Therefore, it is unlikely that LAF3 acts at the level of FHY1 action. The likelihood of a direct effect of LAF3 on COP1 subcellular localization is decreased by the specificity of the hypocotyl phenotype to FR wavelengths. Moreover, the nuclear depletion of COP1 is much slower than the time taken for many of the light-induced changes in photoresponsive gene expression that are compromised in *laf3-1* (von Arnim et al., 1997).

LAF3 Appears to Be an Ortholog of a Ubiquitous Bacterial Protein

Bacteria that contain putative gene products homologous to LAF3 are represented in the Proteobacteria (purple, non-sulfur bacteria), Archaeobacteria, class Firmicutes, Actinobacteria and the Aquificae, Chloroflexi, Fusobacteria, and Thermotogae. Only two of the non-plant LAF3 homologs are predicted to contain transmembrane domains, although with a lower probability than was predicted for the Arabidopsis or rice gene products. In both *Pseudomonas aeruginosa* and *Ralstonia solanacearum*, these predicted regions were found within the first 30 amino acids at the N termini of the proteins.

It is intriguing that LAF3 is homologous to *aepA*, an *Erwinia* sp. gene product that is responsible for regulating enzymes capable of depolymerizing the cell wall and cell wall components. These enzymes facilitate the maceration of host plant tissues and the liberation of nutrients. The *aepA* gene product is believed to regulate the timely induction of these enzymes by responding to levels of specific components of plant extracts to ensure optimal destruction of plant tissues before initiation of the host's defense response (Barras et al., 1994). The homology of LAF3 with this regulatory gene product is consistent with its role in coordinated induction and repression of several phyA-regulated mRNAs (Fig. 1B). Of the phyA-regulated transcripts tested, *XTR7* levels clearly display the strongest regulation by LAF3 (Fig. 1B). *XTR7* transcript abundance correlates well with the extent of inhibition of hypocotyl elongation in different genetic backgrounds and under different light conditions (Fig. 1B). Although like *aepA*, the *XTR7* gene product is also involved in loosening the network of cellulose and xyloglucan fibers in plant cell walls, the reduced sensitivity of *laf3* to FR-induction of genes unrelated to cell wall loosening

(Fig. 1B) argues against a role restricted to regulation cell elongation. It is proposed that coordinated activation of the *aepABH* (activator of extracellular protein production) operon down-regulates expression of the *rsmA* repressor of the synthesis of cell wall-degrading enzymes (Barras et al., 1994), although the precise role of *aepA* action in this process does not appear to have elucidated. Certainly, the ubiquitous presence of *aepA* and *rsmA* homologs throughout microbial kingdoms but not in animals suggests that their roles might extend beyond mediating pathogenicity. It appears that like the phytochromes and His kinase receptors for ethylene and cytokinin, the ancestry of plant LAF3s can be traced back to their prokaryotic heritage and that the functions of LAF3 might have been modified in different species to enhance integration with diverse signaling mechanisms. Notably, *N. crassa* and at least 12 of the bacteria that are predicted to have LAF3 homologs also express putative bacteriophytochrome photoreceptors (Montgomery and Lagarias, 2002). This raises the intriguing possibility that the relationship between LAF3 and phyA signaling may have fairly ancient evolutionary origins. Nonetheless, it is difficult to reconcile the apparently constitutive perinuclear localization of both Arabidopsis LAF3 isoforms with the proposal that *aepA* activates transcription of a pectate lyase gene from *P. carotovorum* (Liu et al., 1993). We cannot eliminate the possibility that the mode of action of LAF3 homologs in bacteria and fungi is distinct from their function(s) in plants.

The use of alternative transcription initiation sites (e.g. Tamaoki et al., 1995), intron splicing sites (Eckardt, 2002), or translational start sites (Chabregas et al., 2003) have all been shown previously to generate isoform diversity in plants. However, pretranslational mechanisms of increasing the flexibility of gene expression by generating alternative products with separable functions do not appear to be used as widely in plants as they are in animal systems. In a time when the availability of genome sequences has led to a strong reliance on the use of predicted ORFs, our unanticipated discovery of two LAF3 isoforms emphasizes the importance of confirming transcript initiation and termination sites to assess possible sources of the fine tuning of biological responses. Although the exact significance of the evolution of distinct transcription initiation sites in the *LAF3* gene is not clear, identification of this locus provides a further contribution to ongoing efforts to interpret plant physiological responses to light in the context of a molecular framework.

MATERIALS AND METHODS

Plant Materials, Growth Conditions, and Genetic Analysis

The *laf3-1* and *phyA-201* mutants are in the Arabidopsis *Ler* background and were compared with WT *Ler-O* in all analyses. The *laf3-1* mutant

corresponds to *Ds*-tagged line GT3069 (Sundaresan et al., 1995). Unless otherwise stated, plant growth conditions and light sources were identical to those described by Bolle et al. (2000). Procedures for mutant screening and PCR-mediated linkage analysis were identical to those described previously (Møller et al., 2001). Cosegregation of the mutant phenotype with transposon-borne genes was confirmed in 120 F₂ seedlings. Seedlings with the *laf* phenotype were rescued from the block in chloroplast development in greening observed in WT plants after transfer from FR_c to W by incubation for 2 d in darkness on Murashige and Skoog medium supplemented with 3% (w/v) Suc before exposure to W.

Molecular Characterization of *laf3-1*

The sequence flanking the transposon in *laf3-1* was cloned by inverse PCR. A 519-bp fragment was amplified using the oligonucleotides 5'-GGTCCGTACGGGATTTTCCC-3' and 5'-CTAAAAAGTGAAAAGGATC-ATGGC-3'. To verify that the cloned genomic region was adjacent to the *Ds* element, a combination of two *Ds* oligonucleotides and two *LAF3* oligonucleotides was used to amplify four fragments spanning the left and right *Ds* borders. Sequence analysis of these fragments confirmed the predicted site of *Ds* integration. The flanking sequence isolated by inverse PCR was used as a probe to screen a flower cDNA library (Weigel et al., 1992) obtained from the Arabidopsis Biological Resource Center (Ohio State University, Columbus). For western analysis, seedlings were ground with a pestle and mortar under liquid nitrogen, and the powder was suspended in 2 volumes of SDS-PAGE sample buffer followed by incubation at 95°C for 5 min. After 10 min of centrifugation, the protein concentrations of the supernatant solutions were quantified using the RC DC protein assay (Bio-Rad, Hercules, CA), and 40 µg of total protein was resolved on 10% (w/v) SDS-PAGE gels before transfer to Immobilon-P nitrocellulose membranes (Bio-Rad). Western blotting was according to standard procedures using the phyA monoclonal antibody mAA1 (Shinomura et al., 1996) and monoclonal anti-actin clone C4 (ICN Biochemicals Inc, Aurora, OH). Levels of phyA and actin were assessed using the ECL PLUS chemiluminescent detection system (Amersham, Buckinghamshire, UK). Northern-blot analysis was conducted as described previously (Møller et al., 2001) using *CHS*, *CAB*, *PET E*, *PET H*, and *XTR7* probes identical to those described elsewhere (Ballesteros et al., 2001; Møller et al., 2001). The 730-bp *ASN1* probe was obtained from a cDNA library by PCR-mediated amplification using the oligonucleotides 5'-GAGGCACAGAGGACCTGACTGG-3' and 5'-GAGCCCTCAAGACCA-ACGCAAAAGG-3'. Comparable RNA loading was verified by ethidium bromide staining and by hybridization with an Arabidopsis 18S rRNA probe.

Cloning the *LAF3* Gene and Complementation Analysis

A bacteriophage-based Arabidopsis genomic library (CLONTECH Laboratories, Palo Alto, CA) from the Columbia ecotype was screened using a 1.3-kb *LAF3* cDNA probe. An 8,067-bp genomic fragment, beginning 3,050 bp upstream of the start codon of the *LAF3*_{ISF1} ORF and encoding 1,293 bp downstream of the stop codon of both *LAF3* isoforms, was excised from one of the isolates by digestion with *XhoI* and *SalI* and cloned into a promoterless binary plant transformation vector (Møller et al., 2001) to generate the construct gLAF3. The entire fragment was sequenced.

To identify the transcription start sites of the *LAF3* gene, 5'-RACE analysis was performed using an Arabidopsis cDNA library generated from 4-d-old etiolated Columbia seedlings using the Marathon cDNA Amplification Kit (CLONTECH Laboratories). Nested gene-specific oligonucleotides used were 5'-GCGTTCAGATGGAATCCAAGCG-3' and 5'-GGGAGGT-ATCTTTTAACCGCG-3'. Three independent fragments corresponding to the 5' termini of *LAF3*_{ISF1} were recovered, and eight independent fragments corresponding to the 5' termini of *LAF3*_{ISF2} were recovered. To test the ability of 35S::*LAF3*_{ISF1} and 35S::*LAF3*_{ISF2} to complement *laf3-1*, full-length *LAF3*_{ISF1} and *LAF3*_{ISF2} cDNAs were amplified by RT-PCR using total RNA isolated from 4-d-old FR_c-irradiated *Ler* seedlings. First strand cDNA was prepared using RNA from etiolated seedlings and the oligonucleotide 5'-GTAAAGTTTGTTCCTTAATTAGATAAAGACTGCATCATC-3' specific to the 3'-untranslated region of both isoforms and M-MLV RT (Invitrogen, Carlsbad, CA) as recommended by the manufacturer. Oligonucleotides used to amplify full-length *LAF3*_{ISF1} from first strand product were 5'-TACTCGAGATGACCGGTTGGTATGAGTTTCC-3' and 5'-GACTAGTCT-

CATGGATACAATTGCTTCTCC-3'. Oligonucleotides used to amplify *LAF3*_{ISF2} were 5'-TACTCGAGATGAACTCTTCGTCAGCGTTTCAGC-3' and 5'-GACTAGTCTCATGGATACAATTGCTTCTCC-3'. The PCR products were sequenced and cloned into the binary transformation vector pBA002 (Kost et al., 1998) under the control of the CaMV 35S promoter. The resulting constructs were transformed into *laf3-1* plants using the *Agrobacterium tumefaciens*-mediated floral dip method and transformants were selected on media containing glufosinate ammonium (BASTA, Crescent Chemical Co., Inc., New York). The progeny from 23 gLAF3 transformants, 65 35S::*LAF3*_{ISF1} transformants, and 63 35S::*LAF3*_{ISF2} transformants were analyzed for restoration of a WT phenotype.

Subcellular Localization of *LAF3* Isoforms

A binary vector YFP-pBA was constructed containing a multicloning site and a full-length YFP cDNA ligated into the *MluI* and *SpeI* sites of pBA002 (Kost et al., 1998). This introduced unique *XhoI*, *AscI*, *MluI*, *PacI*, *AvrII*, *BamHI*, *XmaI*/*SmaI*, and *AatII* sites between the CaMV 35S promoter and YFP in pBA002. Full-length cDNAs encoding *LAF3*_{ISF1} and *LAF3*_{ISF2} were amplified using oligonucleotides that removed the stop codons and cloned as translational fusions to YFP in YFP-pBA. *laf3-1* plants were transformed with the resulting 35S::*LAF3*_{ISF1}-YFP and 35S::*LAF3*_{ISF2}-YFP constructs as described previously, and primary transformants were selected by their resistance to glufosinate ammonium (BASTA, Crescent Chemical Co., Inc.). The progeny of these lines (T₂ generation) was used to assess complementation of the *laf3-1* hypocotyl phenotype in FR_c and to visualize the subcellular localization of *LAF3*_{ISF1}-YFP and *LAF3*_{ISF2}-YFP in root and hypocotyl cells of etiolated seedlings using an inverted TE2000 epifluorescence microscope (Nikon, Tokyo) and Openlab imaging software (Improvision, Coventry, UK).

Mimic-Controlled RT-PCR

The oligonucleotides 5'-AAGTTCAGCATTTGTATCAACTTCCGG-3' and 5'-ATGAACCTTTCGTCATCGTTTCAGCT-3' were both used in conjunction with 5'-CTTGAGAGTGGCAAAGCTTCCAAC-3' to quantify levels of the *LAF3*_{ISF1} and *LAF3*_{ISF2} transcripts, respectively. The *LAF3*_{ISF1}-specific oligonucleotide recognizes part of the 5'-untranslated region of the *LAF3*_{ISF1} transcript beginning 28 nucleotides upstream of the start codon of *LAF3*_{ISF1}. The *LAF3*_{ISF2}-specific oligonucleotide is complementary to the region encoding the first nine amino acids of the *LAF3*_{ISF2} isoform that are spliced out of the primary transcript encoding *LAF3*_{ISF1}. The reverse oligonucleotide common to both RT-PCRs recognizes the sequence encoding the last eight amino acids encoded by the third exon of *LAF3*_{ISF1} (i.e. the second exon of *LAF3*_{ISF2}). Both fragments indicating *LAF3*_{ISF1} and *LAF3*_{ISF2} levels span an intron to eliminate the possibility that genomic DNA contamination interfered with the competition between the target and mimic templates.

The mimics used for *LAF3*_{ISF1} and *LAF3*_{ISF2} transcript quantification were the oligos 5'-AAGTTCAGCATTTGTATCAACTTCCGGTAACGTTGCGTCCAGGGTTGTCACACTGTCTTCTCAGAGCAGATAGTTGACTGACAGGTTGGAAGCTTGGCCACTCTCAAG-3' and 5'-ATGAACCTTTCGTCATCGTTTCAGCGGTTGGGACGAAATCCGTCATACTGTAGTTGTTGTCGTTCTGTGCTGGTTGGAAGCTTGGCCACTCTCAAG-3', respectively. Because the mimic fragments contain the recognition sequences for the amplification oligonucleotides, they compete with target *LAF3*_{ISF1} and *LAF3*_{ISF2} cDNAs during amplification. Fragments specific to both *LAF3*_{ISF1} and *LAF3*_{ISF2} are both approximately 250 bp, whereas fragments arising from amplification of mimics are 110 bp. Artifactual genomic DNA amplifications are predicted to be approximately 400 (for *LAF3*_{ISF1}) and 340 bp (for *LAF3*_{ISF2}) bp.

With the exception of RNA extraction from the seeds (extracted according to Vicent and Delseny, 1999), RNA was extracted using the RNeasy Plant Minikit (Qiagen USA, Valencia, CA). Total RNA samples were treated with RNase-free DNase I (Invitrogen) to eliminate contaminating genomic DNA. After confirmation of RNA integrity by analysis using an Agilent 2100 Bioanalyzer, 3 µg of RNA from each sample was combined with 10 pmol oligo 5'-CTTGAGAGTGGCAAAGCTTCCAAC-3' in a total volume of 10 µL, and the oligo was annealed by heating the sample to 72°C for 2 min before transferring immediately to ice for 2 min. The RT reaction was performed by adding 2 µL of dithiothreitol, 2 µL of dNTP mix (10 mM each),

2 μ L of M-MLV RT (Invitrogen), and 4 μ L of 5 \times buffer provided by the supplier of the enzyme followed by incubation for 1 h at 42°C.

Standard 50- μ L PCRs contained 2 μ L of first strand reaction product, 50 pmol of each amplification oligo, and the appropriate mimic at a predetermined concentration shown to not have reached the limits of amplification after the number of PCR cycles used for the particular set of RNA samples being compared. The RT-PCR runs varied between 18 and 23 cycles (each 94°C for 30 s, 60°C for 30 s, and 72°C for 30 s), depending on the exponential range of amplification. In all cases, identical samples subjected to an additional five cycles were run in parallel to ensure that amplification of the mimic was still in the exponential phase at the time when the sample was withdrawn for use in comparative analyses. Comparable results were obtained when the PCR reaction was repeated once with the same reverse-transcribed sample and twice with an independent reverse-transcribed sample from the same preparations of total RNA. For all experiments, fragments arising from amplification of targets were pooled and sequenced to confirm their identity.

The intensities of bands arising from amplification of *LAF3* transcripts and those arising from amplification of mimics were determined using Quantity One Version 4 image quantification software (Bio-Rad) after image acquisition using a Gel Doc 2000 gel documentation system (Bio-Rad). Comparison of the ratios of the intensities of bands arising from *LAF3* transcripts to bands arising from mimics enabled assessment of the relative levels of the expression of both isoforms.

RT-PCR with the oligonucleotides 5'-TTGCCATTCAGCCGTTCT-TTCT-3' and 5'-ACCCGCAAGATCAAGACGAAGGA-3' was used to ensure comparable starting concentrations of RNA and RT efficiency in all comparisons. These oligonucleotides recognize sites that span the second intron in the *ACTIN2* gene (At5g09810) to amplify a 147-bp fragment from correctly spliced mRNA transcripts. First strand cDNA was synthesized by priming using the latter oligonucleotide.

Distribution of Materials

Upon request, all novel materials described in this publication will be made available in a timely manner for noncommercial research purposes, subject to the requisite permission from any third party owners of all or parts of the material. Obtaining any permission will be the responsibility of the requestor.

ACKNOWLEDGMENTS

We are grateful to Venkatesan Sundaresan for providing *Ds*-tagged lines, Qi-Wen Niu for mutant screening, Mathias Zeidler for the cDNA used for 5'-RACE analysis, and Akira Nagatani for phyA antibody.

Received June 12, 2003; returned for revision July 2, 2003; accepted August 28, 2003.

LITERATURE CITED

- Amador V, Monte E, García-Martínez J-L, Prat S (2001) Gibberellins signal nuclear import of PHOR1, a photoperiod-responsive protein with homology to *Drosophila* armadillo. *Cell* **106**: 343–354
- Ballesteros ML, Bolle C, Lois LM, Moore JM, Vielle-Calzada J-P, Grossniklaus U, Chua N-H (2001) LAF1, a MYB transcription activator for phytochrome A signaling. *Genes Dev* **15**: 2613–2625
- Barnes SA, Nishizawa NK, Quaggio RB, Whitelam GC, Chua N-H (1996a) Far red light blocks greening of *Arabidopsis* seedlings via a phytochrome A-mediated change in plastid development. *Plant Cell* **8**: 601–615
- Barnes SA, Quaggio RB, Whitelam GC, Chua N-H (1996b) *flh1* defines a branch point in phytochrome A signal transduction pathways for gene expression. *Plant J* **10**: 1155–1161
- Barras F, van Gijsegem F, Chatterjee AK (1994) Extracellular enzymes and pathogenesis of soft-rot *Erwinia*. *Annu Rev Phytopathol* **32**: 201–234
- Bolle C, Koncz C, Chua N-H (2000) PAT1, a new member of the GRAS family, is involved in phytochrome A signal transduction. *Genes Dev* **14**: 1269–1278
- Bowler C, Neuhaus G, Yamagata H, Chua N-H (1994) Cyclic GMP and calcium mediate phytochrome phototransduction. *Cell* **77**: 73–81
- Büche C, Poppe C, Schäfer E, Kretsch T (2000) *eid1*: a new *Arabidopsis* mutant hypersensitive in phytochrome A-dependent high-irradiance responses. *Plant Cell* **12**: 547–558

- Cantón FR, Quail PH (1999) Both phyA and phyB mediate light-imposed repression of *PHYA* gene expression in *Arabidopsis*. *Plant Physiol* **121**: 1207–1216
- Carmo-Fonseca M (2002) The contribution of nuclear compartmentation to gene regulation. *Cell* **108**: 513–521
- Chabregas SM, Luche DD, van Sluys M-A, Menck CFM, Silva-Filho MC (2003) Differential usage of two in-frame translational start codons regulates subcellular localization of *Arabidopsis thaliana* TH11. *J Cell Sci* **116**: 285–291
- Choi G, Yi H, Lee J, Kwon Y-K, Sho MS, Shin B, Luka Z, Hahn T-R, Song P-S (1999) Phytochrome signaling is mediated through nucleoside diphosphate kinase 2. *Nature* **401**: 610–613
- Cólon-Carmona A, Chen DL, Yeh K-C, Abel S (2000) Aux/IAA proteins are phosphorylated by phytochrome *in vitro*. *Plant Physiol* **124**: 1728–1738
- Desnos T, Puente P, Whitelam GC, Harberd NP (2001) FHY1: a phytochrome A-specific signal transducer. *Genes Dev* **15**: 2980–2990
- Dieterle M, Zhou Y-C, Schäfer E, Funk M, Kretsch T (2001) EID1, an F-box protein involved in phytochrome A-specific light signaling. *Genes Dev* **15**: 939–944
- Eckardt NA (2002) Alternative splicing and the control of flowering time. *Plant Cell* **14**: 743–747
- Fairchild CD, Schumaker MA, Quail PH (2000) HFR1 encodes an atypical bHLH protein that acts in phytochrome A signal transduction. *Genes Dev* **14**: 2377–2391
- Fankhauser C, Chory J (2000) *RSF1*, an *Arabidopsis* locus implicated in phytochrome A signaling. *Plant Physiol* **124**: 39–45
- Fankhauser C, Yeh K-C, Lagarias JC, Zhang H, Elich TD, Chory J (1999) PKS1, a substrate phosphorylated by phytochrome that modulates light signaling in *Arabidopsis*. *Science* **284**: 1539–1541
- Guo H, Mockler T, Duong H, Lin C (2001) SUB1, an *Arabidopsis* Ca²⁺-binding protein involved in cryptochrome and phytochrome action. *Science* **291**: 487–490
- Heerklotz D, Doring P, Bonzelius F, Winkelhaus S, Nover L (2001) The balance of nuclear import and export determines the intracellular distribution and function of tomato heat stress transcription factor HsfA2. *Mol Cell Biol* **21**: 1759–1768
- Hoecker U, Tepperman JM, Quail PH (1999) SPA1, a WD-repeat protein specific to phytochrome A signal transduction. *Science* **284**: 496–499
- Hsieh HL, Okamoto H, Wang M, Ang LH, Matsui M, Goodman H, Deng X-W (2000) FIN219, an auxin-regulated gene, defines a link between phytochrome A and the downstream regulator COP1 in light control of *Arabidopsis* development. *Genes Dev* **14**: 1958–1970
- Hu J, Aguirre M, Peto C, Alonso J, Ecker J, Chory J (2002) A role for peroxisomes in photomorphogenesis and development of *Arabidopsis*. *Science* **297**: 405–409
- Hudson M, Ringli C, Boylan MT, Quail PH (1999) The *FAR1* locus encodes a novel nuclear protein specific to phytochrome A signaling. *Genes Dev* **13**: 2017–2027
- Igarashi D, Ishida S, Fukazawa J, Takahashi Y (2001) 14–3-3 proteins regulate intracellular localization of the bZIP transcriptional activator RSG. *Plant Cell* **13**: 2483–2497
- Johnson E, Bradley M, Harberd NP, Whitelam GC (1994) Photoresponses of light-grown *phyA* mutants of *Arabidopsis*: phytochrome A is required for the perception of daylength extensions. *Plant Physiol* **105**: 141–149
- Kang J-G, Ju Y, Kim D-H, Chung K-S, Fujioka S, Kim J-I, Dae H-W, Yoshida S, Takatsuto S, Song P-S et al. (2001) Light and brassinosteroid signals are integrated via a dark-induced small G-protein in etiolated seedling growth. *Cell* **105**: 625–636
- Kim D-H, Kang J-G, Yang S-S, Chung K-S, Song P-S, Park C-M (2002) A phytochrome-associated protein phosphatase 2A modulates light signals in flowering time control in *Arabidopsis*. *Plant Cell* **14**: 3043–3056
- Kircher S, Wellmer F, Nick P, Rügner A, Schäfer E, Harter K (1999) Nuclear import of the parsley bZIP transcription factor CPRF2 is regulated by phytochrome photoreceptors. *J Cell Biol* **144**: 201–211
- Kost B, Spielhofer P, Chua N-H (1998) A GFP-mouse talin fusion protein labels plant actin filaments *in vivo* and visualizes the actin cytoskeleton in growing pollen tubes. *Plant J* **16**: 393–401
- Liu Y, Murata H, Chatterjee A, Chatterjee AK (1993) Characterization of a novel regulatory gene *aepA* that controls extracellular enzyme production in the phytopathogenic bacterium *Erwinia carotovora* subsp. *carotovora*. *Mol Plant-Microbe Interact* **6**: 299–308

- Ma L, Li J, Qu L, Hager J, Chen Z, Zhao H, Deng X-W (2001) Light control of *Arabidopsis* development entails coordinated regulation of genome expression and cellular pathways. *Plant Cell* **13**: 2589–2607
- Møller SG, Ingles PJ, Whitelam GC (2002) The cell biology of phytochrome signaling. *New Phytol* **154**: 553–590
- Møller SG, Kunkel T, Chua N-H (2001) A plastidic ABC protein involved in intercompartmental communication of light signaling. *Genes Dev* **15**: 90–103
- Montgomery BL, Lagarias JC (2002) Phytochrome ancestry: sensors of bilins and light. *Trends Plant Sci* **7**: 357–366
- Nagy F, Schäfer E (2002) Phytochromes control photomorphogenesis by differentially regulated, interacting signaling pathways in higher plants. *Annu Rev Plant Biol* **53**: 329–355
- Osterlund MT, Deng X-W (1998) Multiple photoreceptors mediate the light-induced reduction of GUS-COP1 from *Arabidopsis* hypocotyl nuclei. *Plant J* **16**: 201–208
- Osterlund MT, Hardtke CS, Wei N, Deng X-W (2000) Targeted destabilization of HY5 in light development of *Arabidopsis*. *Nature* **405**: 462–466
- Rose A, Meier I (2001) A domain unique to plant RanGAP is responsible for its targeting to the plant nuclear rim. *Proc Natl Acad Sci USA* **98**: 15377–15382
- Seo HS, Yang J-Y, Ishikawa M, Bolle C, Ballesteros ML, Chua N-H (2003) LAF1 ubiquitination by COP1 controls photomorphogenesis and is stimulated by SPA1. *Nature* **423**: 995–999
- Sharrock RA, Clack T (2002) Patterns of expression and normalized levels of the five *Arabidopsis* phytochromes. *Plant Physiol* **130**: 442–456
- Shinomura T, Nagatani A, Hanzawa H, Kubota M, Watanabe M, Furuya M (1996) Action spectra for phytochrome A- and B-specific photoinduction of seed germination in *Arabidopsis thaliana*. *Proc Natl Acad Sci USA* **93**: 8129–8133
- Soh M-S, Kim Y-M, Han S-J, Song P-S (2000) REP1, a basic helix-loop-helix protein, is required for a branch pathway of phytochrome A signaling in *Arabidopsis*. *Plant Cell* **12**: 2061–2073
- Stone SL, Anderson EM, Mullen RT, Goring DR (2003) ARC1 is an E3 ubiquitin ligase and promotes the ubiquitination of proteins during the rejection of self-incompatible *Brassica* pollen. *Plant Cell* **15**: 885–898
- Sundaresan V, Springer P, Volpe T, Haward S, Jones JDG, Dean C, Ma H, Martienssen R (1995) Patterns of gene action in plant development revealed by enhancer trap and gene trap transposable elements. *Genes Dev* **9**: 1797–1810
- Tamaoki M, Tsugawa H, Minami E, Kayano T, Yamamoto N, Kano-Murakami Y, Matsuoka M (1995) Alternative RNA products from a rice homeobox gene. *Plant J* **7**: 927–938
- Tepperman JM, Zhu T, Chang H-S, Wang X, Quail PH (2001) Multiple transcription factor genes are early targets of phytochrome A signaling. *Proc Natl Acad Sci USA* **98**: 9437–9442
- Thum KE, Kim M, Christopher DA, Mullet JE (2001) Cryptochrome 1, cryptochrome 2, and phytochrome A co-activate the chloroplast *psbD* blue light-responsive promoter. *Plant Cell* **13**: 2747–2760
- Vicent CM, Delseny M (1999) Isolation of total RNA from *Arabidopsis thaliana* seeds. *Anal Biochem* **268**: 412–413
- von Arnim A, Osterlund MT, Kwok SF, Deng X-W (1997) Genetic and developmental control of nuclear accumulation of COP1, a repressor of photomorphogenesis in *Arabidopsis*. *Plant Physiol* **114**: 779–788
- Wang H, Deng XW (2002) *Arabidopsis* FHY3 defines a key phytochrome A signaling component directly interacting with its homologous partner FAR1. *EMBO J* **21**: 1339–1349
- Wang H, Ma L, Habashi J, Li J, Zhao H, Deng X-W (2002) Analysis of far-red light-regulated genome expression profiles of phytochrome A pathway mutants in *Arabidopsis*. *Plant J* **32**: 723–733
- Weigel D, Alvarez J, Smyth DR, Yanofsky MF, Meyerowitz EM (1992) LEAFY controls floral meristem identity in *Arabidopsis*. *Cell* **69**: 843–859
- Yanovsky MJ, Kay SA (2002) Molecular basis of seasonal time measurement in *Arabidopsis*. *Nature* **419**: 308–312
- Yeh K-C, Lagarias JC (1998) Eukaryotic phytochromes: light-regulated serine/threonine protein kinases with histidine kinase ancestry. *Proc Natl Acad Sci USA* **95**: 13976–13981
- Zeidler M, Bolle C, Chua N-H (2001) The phytochrome A specific component PAT3 is a positive regulator of *Arabidopsis* photomorphogenesis. *Plant Cell Physiol* **42**: 1193–1200